

Electronic Supplementary Information (ESI)

Polar and Tropical Regioisomeric Decanuclear Cuprofullerenes

Jing-Xuan Sun,^{a†} Ting-Ting Zou,^{a†} Yi-Chun Zhang,^a Yu-Li Liu,^a Li Dang,^a Shun-Ze Zhan,^{*a}
Hong Cai,^{*c} Dan Li^{*b}

Abstract: Achieving exohedral metallofullerenes (ExMFs) with metal atoms selectively binding at specific spatial positions on the surface of a C₆₀ molecule remains a considerable challenge. In this study, we report the synthesis of two decanuclear, regioisomeric cuprofullerenes with polar and tropical coordination patterns. Complex **1** features 10 Cu^I atoms coordinated to the C=C bonds of two polar zones, stabilized by Cl⁻ anions and protonated 4-methoxybenzylamine counteranions. Complex **2** involves coordination of 10 Cu^I atoms in the tropical zone, utilizing trifluoroacetate (**L_F**) and 5-methylpicolinate (**L_{mpic}**) as auxiliary ligands. Notably, complex **2** forms a typical *pcu* topology MOF, linking tropical cuprofullerenes through Cu^{II}(**L_{mpic}**)₂ units. Theoretical calculations reveal intricate charge transfer processes that significantly influence electronic properties of these cuprofullerenes.

[a] J.-X. Sun, T.-T. Zou, Y.-C. Zhang, Y.-L. Liu, Prof. Dr. L. Dang, Prof. Dr. S.-Z. Zhan
College of Chemistry and Chemical Engineering, and Key (Guangdong-Hong Kong Joint)
Laboratory for Preparation and Application of Ordered Structural Materials of Guangdong
Province
Shantou University
Shantou 515063, P. R. China
E-mail: szzhan@stu.edu.cn

[b] Prof. Dr. D. Li
College of Chemistry and Materials Science and Guangdong Provincial Key Laboratory of
Supramolecular Coordination Chemistry
Jinan University
Guangzhou 510632, P. R. China
E-mail: danli@jnu.edu.cn

[c] Prof. Dr. H. Cai,
School of Chemistry and Environmental Engineering
Hanshan Normal University
Chaozhou 521041, P. R. China.
E-mail: tiddychen@163.com

[†]J.-X. Sun and T.-T. Zou contributed equally to this work.

Table of Contents

1. Experimental Procedures	2
1.1 Materials and Physical Measurements	2
1.2 Synthesis.....	2
1.3 Crystal Structural Determination	3
2. Results and Discussion	4
2.1 Crystal Data.....	4
2.2 Additional Structural Description	7
3. Theoretical Calculation Details.....	10
3.1 Time Dependent Density Functional Theory (TD-DFT) Calculation.....	10
4. References.....	20

1. Experimental Procedures

1.1 Materials and Physical Measurements

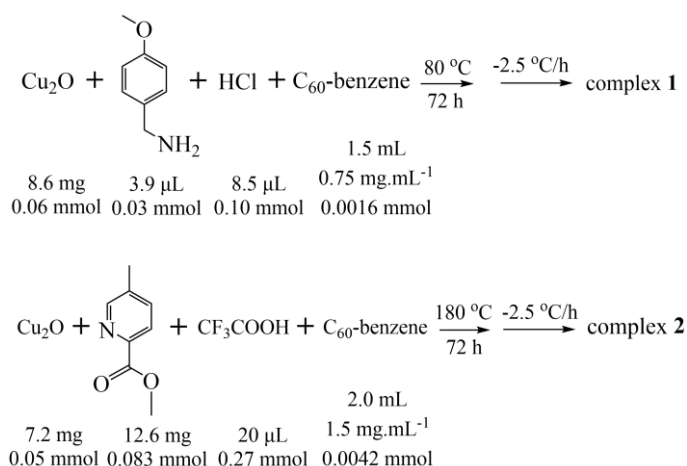
Commercially available starting materials and solvents were used without further purification. C₆₀ (99.5%) was purchased from Xiamen Funano New Material Technology Company LTD without purifications. Thermogravimetric analysis (TGA) was performed on a TA Instruments Q50 Thermogravimetric Analyzer under a nitrogen flow of 40 mL·min⁻¹ at a heating rate of 20 °C·min⁻¹. Powder X-ray diffraction (PXRD) experiment was performed on a MiniFlex 600 X-ray diffractometer of Rigaku Corporation. Infrared spectrum (IR) was obtained in KBr pellet on a Nicolet Avatar 360 FTIR spectrometer in the range of 4000–500 cm⁻¹; abbreviations used for the IR bands are: w = weak, m = medium, s = strong, vs = very strong. The diffuse reflectance solid-state UV-Vis spectra of these complexes were obtained on a Lambda950 UV/Vis/NIR spectrophotometer of Perkin Elmer using pure powder sample and pure BaSO₄ as background. X-ray photoelectron spectroscopy (XPS) was performed on a PHI5000 VersaProbe III (ULVAC-PHI, INC).

1.2 Synthesis

Complex 1: A mixture of Cu₂O (8.6 mg, 0.06 mmol), 4-methoxybenzylamine (3.9 μL, 0.03 mmol), HCl (0.10 mmol, 8.5 μL) and C₆₀ benzene solution (0.0016 mmol, 1.5 mL, 0.75 mg·mL⁻¹) were sealed into Pyrex tube with an inner diameter of 8.0 mm and a capacity of 6.0 mL. Then the tube was heated at 80 °C in a programmable oven for

72 h and cooled to room temperature at the rate of $-2.5\text{ }^{\circ}\text{C}\cdot\text{h}^{-1}$. Black tinny needle-like crystals were separated mechanically in 15% yields based on C_{60} .

Complex 2: A mixture of Cu_2O (7.2 mg, 0.05 mmol), methyl 5-methylpicolinate (12.6 mg, 0.083 mmol), trifluoroacetic acid (20 μL , 0.27 mmol,) and C_{60} benzene solution (0.0042 mmol, 2.0 mL, $1.5\text{ mg}\cdot\text{mL}^{-1}$) were sealed into Pyrex tube with an inner diameter of 8.0 mm and a capacity of 6.0 mL. Then the tube was heated at $180\text{ }^{\circ}\text{C}$ in a programmable oven for 72 h and cooled to room temperature at the rate of $-2.5\text{ }^{\circ}\text{C}\cdot\text{h}^{-1}$. Black block crystals were separated mechanically in 25% yields based on C_{60} .



Scheme S1 Synthesis reactions of the cuprofullerene complexes **1** and **2**.

1.3 Crystal Structural Determination

Single crystal X-ray data collection for the materials was performed on a Rigaku OD (Enhance Cu X-ray Source, $K\alpha$, $\lambda = 1.54184\text{ \AA}$) with CCD Plate (XtaLAB Pro: Kappa single) under 100 K. Data were processed with the CrysAlisPro 1.171.39.28b (Rigaku Oxford Diffraction, 2015). Structures were solved by direct methods by ShelXS^[1] in Olex2 1.2^[2] and refined on F^2 using full-matrix least-squares (SHELXL-2017/1^[1] in Olex2 1.2^[2]). All non-hydrogen atoms were refined with anisotropic thermal parameters. Crystal data and structure refinement for the complexes were summarized in Table S1. Selected bond lengths and angles were given in Table S2-S6.

2. Results and Discussion

2.1 Crystal Data

Table S1 Crystal data and structure refinements for the complexes **1** and **2**.

Complexes	1	2
CCDC	2300702	2358411
Chemical formula	C ₁₄₈ H ₁₄₂ Cl ₂₁ Cu ₁₀ N ₁₁ O ₁₆	C ₁₆₄ H ₇₈ Cu ₁₃ F ₃₀ N ₆ O ₃₂
Formula weight	3710.57	4040.34
Crystal system	Triclinic	Triclinic
Space group	<i>P</i> -1	<i>P</i> -1
a (Å)	12.1936(2)	15.5866(4)
b (Å)	17.4981(4)	16.3903(5)
c (Å)	17.5483(3)	16.9027(4)
α (deg)	101.9784(16)	103.034(2)
β (deg)	92.5479(13)	112.931(2)
γ (deg)	96.2693(16)	99.251(2)
V (Å ³)	3632.07(12)	3722.69(18)
Z	1	1
D _{calcd} (g·cm ⁻³)	1.696	1.802
Reflections collected	45731	38223
Unique reflections	14557	13503
R _{int}	0.0426	0.0298
GOOF	1.054	1.021
R ₁ ^a [I > 2σ(I)]	0.0481	0.0534
wR ₂ ^b [I > 2σ(I)]	0.1166	0.1435
R ₁ ^a [all refl.]	0.0649	0.0669
wR ₂ ^b [all refl.]	0.1245	0.1547

$$^a R_1 = \sum (||F_o| - |F_c||) / \sum |F_o|, \quad ^b wR_2 = [\sum w(F_o^2 - F_c^2)^2 / \sum w(F_o^2)^2]^{1/2}.$$

Table S2 Selected bond lengths (Å) in complex **1**.

Bond length (Å)			
Cu-Cu			
Cu1-Cu2	3.4641(5)	Cu2-Cu3	3.6829(6)
Cu3-Cu4	3.6495(6)	Cu4-Cu5	3.4518(5)
Cu1-Cu5	3.4788(5)		
Cu-Cl			
Cu1-Cl1	2.3511(1)	Cu1-Cl2	2.4218(1)
Cu1-Cl6	2.2818(2)	Cu2-Cl2	2.3820(2)
Cu2-Cl3	2.3719(1)	Cu2-Cl7	2.3047(1)
Cu3-Cl3	2.3762(1)	Cu3-Cl4	2.3604(1)
Cu3-Cl8	2.2652(1)	Cu4-Cl4	2.3948(1)
Cu4-Cl5	2.4006(1)	Cu4-Cl9	2.2745(1)
Cu5-Cl11	2.3708(2)	Cu5-Cl5	2.4132(1)
Cu5-Cl10	2.2455(5)		
Cu-C			
Cu1-C21	2.134(4)	Cu1-C22	2.061(4)
Cu2-C25	2.082(3)	Cu2-C30	2.146(4)
Cu3-C28	2.043(3)	Cu3-C29	2.194(3)
Cu4-C18	2.072(3)	Cu4-C19	2.135(3)
Cu5-C3	2.042(3)	Cu5-C20	2.096(3)

C=C (coordinated hexagons)			
(6,6)			
C21-C22	1.418(5)	C25-C30	1.423(5)
C28-C29	1.420(5)	C18-C19	1.420(5)
C3-C20	1.433(5)		

Table S3 Selected Cl...H distances (Å) in complex **1**.

Cl9-H6C	2.5010(4)	Cl8-H6B	2.9332(5)
Cl8-H5B	2.3600(4)	Cl8-H2C	2.4595(4)
Cl7-H3B	2.6222(4)	Cl7-H3A	2.3883(4)
Cl6-H3C	2.4342(4)	Cl6-H1C	2.3360(3)
Cl5-H6C	2.8703(4)	Cl5-H4C	2.5268(4)
Cl4-H5B	2.8021(4)	Cl4-H4A	2.5611(4)
Cl3-H4A	2.8118(4)	Cl3-H2C	2.8142(4)
Cl2-H4B	2.4453(4)	Cl2-H3B	2.7670(4)
Cl11-H6A	2.3723(4)	Cl11-H5C	2.3738(4)
Cl10-H6B	2.4041(4)	Cl10-H2A	2.5064(4)
Cl1-H2A	2.8258(4)		

Table S4 Selected bond angles (°) in complex **1**.

Bond angle (°)			
Cl-Cu-Cl			
Cl1-Cu1-Cl2	98.26(4)	Cl6-Cu1-Cl1	106.16(4)
Cl6-Cu1-Cl2	105.30(5)	Cl3-Cu2-Cl2	102.70(4)
Cl7-Cu2-Cl2	98.60(4)	Cl7-Cu2-Cl3	109.03(4)
Cl4-Cu3-Cl3	109.92(4)	Cl8-Cu3-Cl3	108.17(4)
Cl8-Cu3-Cl4	103.50(4)	Cl4-Cu4-Cl5	100.19(4)
Cl9-Cu4-Cl4	109.35(4)	Cl9-Cu4-Cl5	100.73(4)
Cl1-Cu5-Cl5	97.18(4)	Cl10-Cu5-Cl1	103.90(4)
Cl10-Cu5-Cl5	104.76(4)		
C-Cu-Cl			
C21-Cu1-Cl1	102.51(10)	C21-Cu1-Cl2	99.44(9)
C21-Cu1-Cl6	138.54(10)	C22-Cu1-Cl1	121.33(10)
C22-Cu1-Cl2	124.56(10)	C22-Cu1-Cl6	99.32(11)
C25-Cu2-Cl2	126.90(10)	C25-Cu2-Cl3	113.97(10)
C25-Cu2-Cl7	103.80(10)	C30-Cu2-Cl2	100.78(10)
C30-Cu2-Cl3	98.15(10)	C30-Cu2-Cl7	142.01(10)
C28-Cu3-Cl3	115.51(11)	C28-Cu3-Cl4	118.33(10)
C28-Cu3-Cl8	99.62(10)	C29-Cu3-Cl3	96.83(10)
C29-Cu3-Cl4	98.10(9)	C29-Cu3-Cl8	138.51(10)
C18-Cu4-Cl4	115.30(10)	C18-Cu4-Cl5	126.71(10)
C18-Cu4-Cl9	103.07(11)	C19-Cu4-Cl4	98.40(9)
C19-Cu4-Cl5	99.91(10)	C19-Cu4-Cl9	141.54(10)
C3-Cu5-Cl1	122.13(11)	C3-Cu5-Cl5	125.77(10)
C3-Cu5-Cl10	100.40(10)	C20-Cu5-Cl1	102.92(11)
C20-Cu5-Cl5	99.79(9)	C20-Cu5-Cl10	140.69(10)
C-Cu-C			
C22-Cu1-C21	39.48(13)	C25-Cu2-C30	39.29(13)
C28-Cu3-C29	38.97(14)	C18-Cu4-C19	39.42(14)
C3-Cu5-C20	40.48(13)		

Table S5 Selected bond lengths (Å) in complex **2**.

Bond length (Å)			
Cu-Cu			
Cu1-Cu2	3.4860(7)	Cu2-Cu3	3.0814(7)
Cu3-Cu4	3.6666(8)	Cu4-Cu5	3.0798(7)
Cu1-Cu5	3.4860(7)		
Cu-O			
Cu1-O1	1.9614(4)	Cu1-O11	1.9538(7)
Cu1-O13	2.2742(4)	Cu2-O3	1.9981(4)
Cu2-O5	1.9539(3)	Cu2-O13	2.2004(3)
Cu3-O4	1.9461(2)	Cu3-O6	2.2885(9)
Cu3-O15	2.02546(1)	Cu4-O7	1.9999(1)
Cu4-O9	1.9666(4)	Cu4-O16	2.4667(5)
Cu5-O8	1.9828(3)	Cu5-O10	2.2379(6)
Cu5-O2	1.9826(4)	Cu6-O12	1.9450(1)
Cu7-O16	1.9444(9)	Cu8-O14	1.9124(1)
Cu-N			
Cu6-N1	1.9629(2)	Cu7-N3	1.9566(1)
Cu8-N2	1.9481(1)		
Cu-C			
Cu1-C1	2.0025(5)	Cu1-C2	2.0043(9)
Cu2-C20	1.9693(4)	Cu2-C21	2.0529(4)
Cu3-C24	1.9886(4)	Cu3-C30	2.0405(1)
Cu4-C25	2.0656(4)	Cu4-C26	1.9655(4)
Cu5-C10	2.0264(8)	Cu5-C11	2.0160(6)
C-C (coordinated hexagons)			
C1-C2	1.4298(3)	C20-C21	1.4204(3)
C24-C30	1.4369(3)	C25-C26	1.4273(3)
C10-C11	1.4354(3)		

Table S6 Selected bond angles (°) in complex **2**.

O-Cu-O			
O1-Cu1-O13	92.45(11)	O11-Cu1-O1	104.56(13)
O11-Cu1-O1	104.56(13)	O11-Cu1-O13	85.57(12)
O3-Cu2-O13	92.24(12)	O5-Cu2-O3	101.47(17)
O5-Cu2-O13	99.81(12)	O4-Cu3-O6	99.02(13)
O4-Cu3-O15	98.97(12)	O15-Cu5-O6	83.48(11)
O16-Cu6-O16#3	180.0	O7-Cu4-O9	97.34(13)
O8-Cu5-O10	96.14(13)		
O-Cu-N			
O12-Cu1-N1	84.02(13)	O12-Cu1-N1#1	95.98(13)
O12#1-Cu1-N1	95.98(13)	O12#1-Cu1-N1#1	84.02(13)
O14-Cu3-N2	84.65(14)	O14-Cu3-N2#2	95.35(14)
O14#2-Cu3-N2	95.35(14)	O14#2-Cu3-N2#2	84.65(14)
O16-Cu6-N3	83.25(13)	O16-Cu6-N3#3	96.75(13)
O16#3-Cu6-N3	96.75(13)	O16#3-Cu6-N3#3	83.25(13)
O-Cu-C			
O1-Cu2-C1	109.34(15)	O11-Cu2-C2	103.16(15)
O13-Cu2-C1	103.39(14)	O13-Cu4-C20	103.47(14)
O13-Cu4-C21	97.43(13)	O3-Cu4-C20	102.96(16)
O5-Cu4-C21	110.55(17)	O4-Cu5-C30	105.84(15)
O6-Cu5-C24	103.71(14)	O15-Cu5-C30	144.48(14)
O15-Cu5-C24	107.53(14)	O7-Cu7-C26	105.56(14)
O9-Cu7-C25	113.91(15)	O8-Cu8-C11	104.50(14)
O10-Cu8-C10	104.10(15)		
C-N-Cu			
C42-N1-Cu1	111.8(3)	C49-N2-Cu3	111.4(3)
C56-N3-Cu6	112.1(3)		

C-Cu-C			
C1-Cu2-C2	41.82(17)	C20-Cu4-C21	41.30(16)
C24-Cu5-C30	41.76(16)	C25-Cu7-C26	41.39(16)
C10-Cu8-C11	41.60(16)		
C-O-Cu			
C31-O1-Cu2	124.8(3)	C41-O11-Cu2	127.8(3)
C48-O13-Cu2	119.2(3)	C33-O3-Cu4	129.4(3)
C33-O4-Cu5	111.5(3)	C55-O15-Cu5	110.4(3)
C37-O7-Cu7	125.7(3)	C39-O9-Cu7	109.9(3)
Symmetry codes			
#1: 2-x, 2-y, 2-z; #2: 1-x, 2-y, 1-z; #3: 1-x, 1-y, -z; #4: 1-x, 1-y, 1-z			

2.2 Additional Structural Description

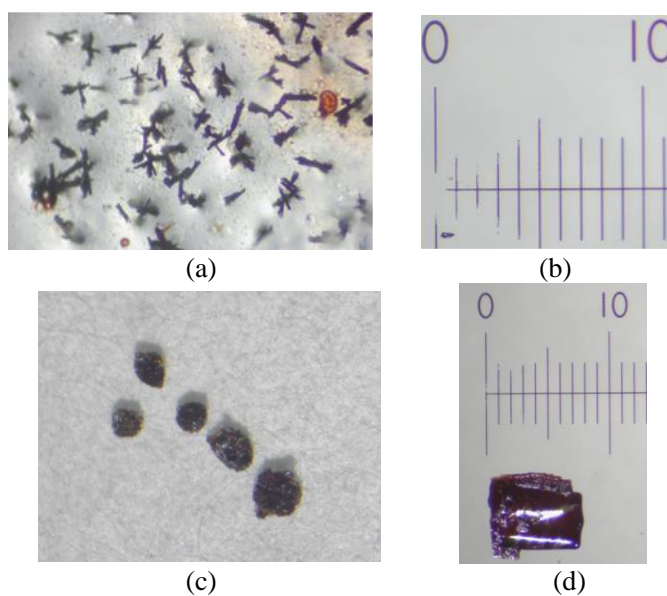


Fig. S1 Crystal images of cuprofullerene complexes **1** (ab) and **2** (cd) amplified 40 times under a microscope. (bd) Crystal images on a scale with the minimum scale of 0.1 mm.

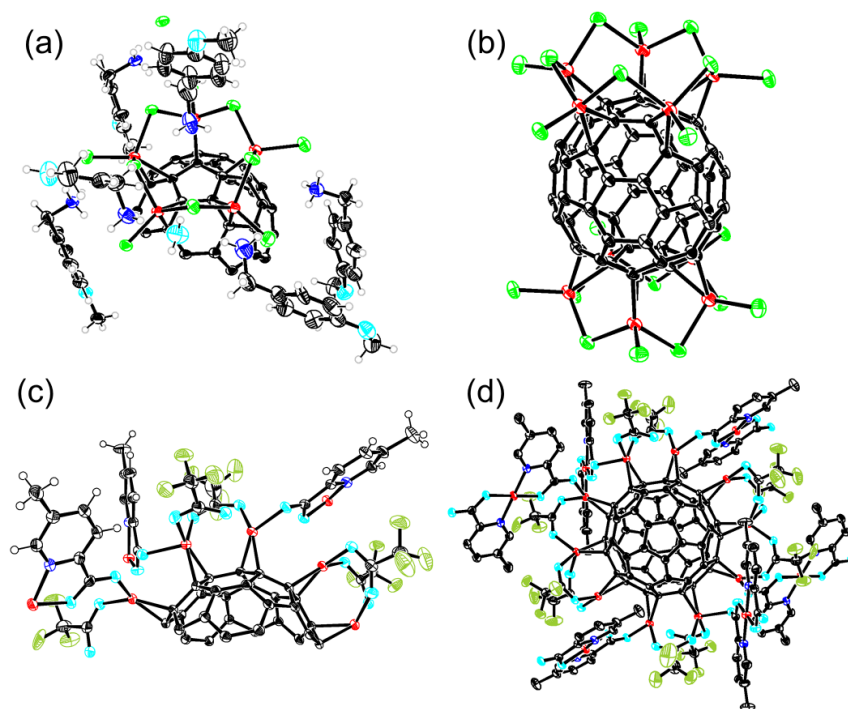


Fig. S2 Asymmetrical units (left, ac) and fragment structures (right, bd) of the complex **1** (ab) and **2** (cd) with 50% thermal ellipsoid. (Color code: red, Cu; green, Cl; black, C; blue, N; cyan, O; yellow green, F.)

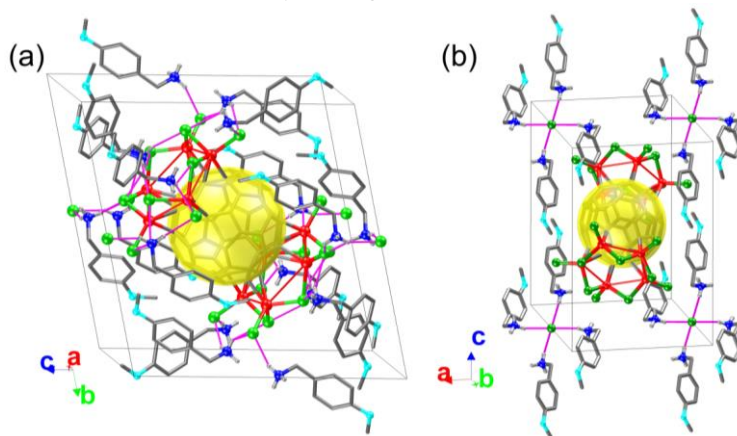
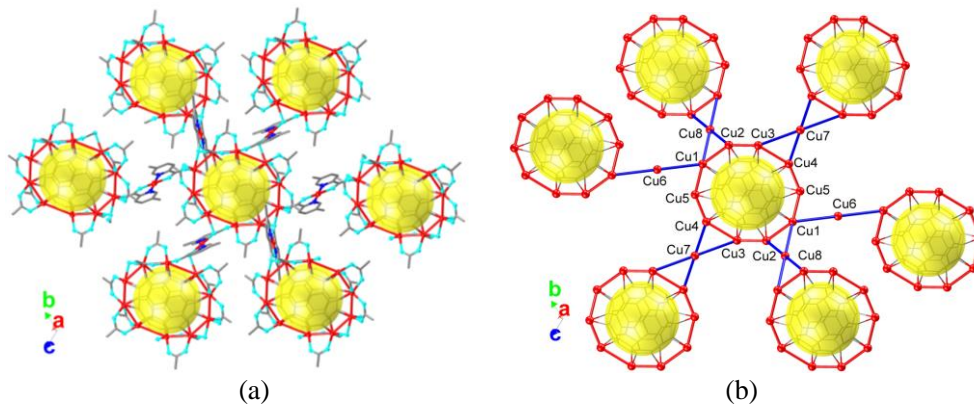


Fig. S3 H...Cl weak interactions (pink line) between -NH_3^+ cations and coordinating Cl (a) and crystallized Cl (b) anions. (Color code: red, Cu; green, Cl; black, C; blue, N; cyan, O; H, grey.)



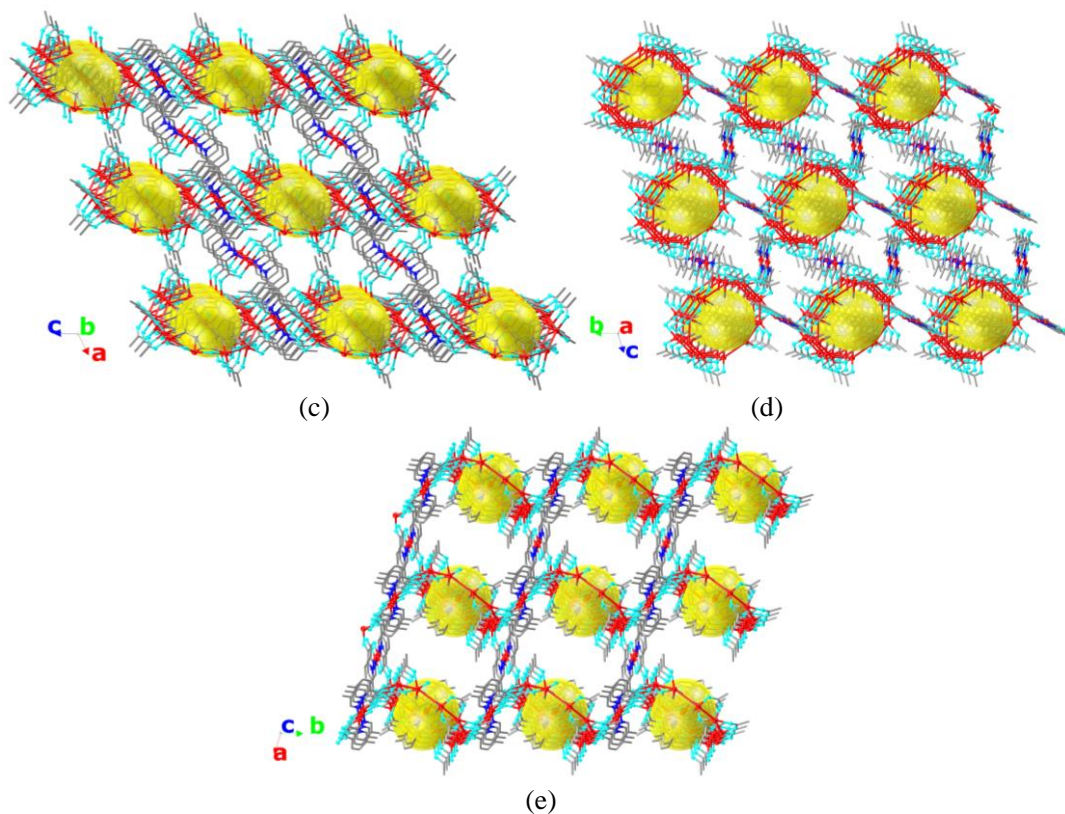


Fig. S4 3D packing structures of complex **2** showing the connection between the decanuclear tropic cuprofullerenes (ab) and the vacant space (c-e) along a , b and c axis. The crystallized benzene molecules are omitted for clarity.

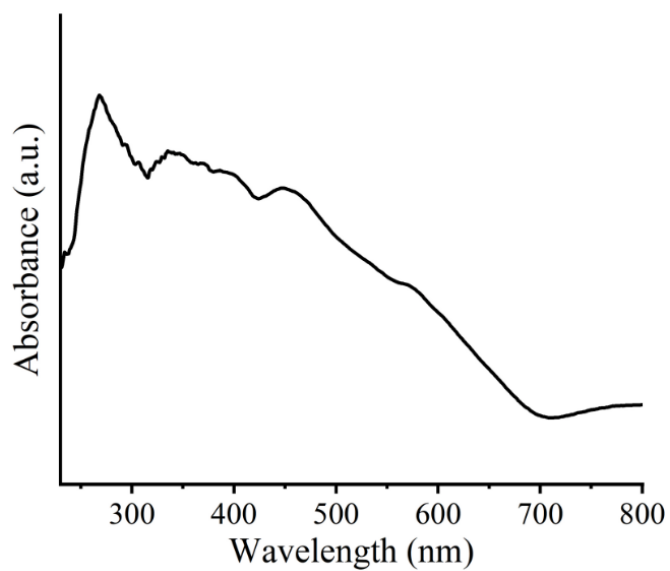


Fig. S5 Diffuse reflectance solid-state UV-Vis spectra of complex **2**.

3. Theoretical Calculation Details

3.1 Time Dependent Density Functional Theory (TD-DFT) Calculation

As shown in Fig. S6, the calculated models of the decanuclear cuprofullerene units were selected from the crystal structures with chemical composition of $[(\text{Cu}^{\text{I}}_5\text{Cl}_{10})(\text{C}_{60})(\text{Cu}^{\text{I}}_5\text{Cl}_{10})]^{10-} \cdot 10(\text{C}_8\text{H}_{12}\text{NO})^+$ (complex **1**, Fig. S6a) and $\text{Cu}^{\text{I}}_{10}\text{C}_{60}(\text{CF}_3\text{COO})_{10}(\text{C}_7\text{H}_7\text{NO}_2)_6$ (complex **2**, Fig. S6b). All the calculations were carried out with Gaussian 16 software package.^[8] No optimization was performed for the calculated model. The exact-exchange-incorporated PBE0 hybrid functional^[9] was employed throughout with LANDL2DZ basis set^[10] for Cu atoms, 6-31G* basis set for C, O, N, F, H and Cl.^[11] To perform wavefunction analysis, some of the out files were used as input files of Multiwfn software packages.^[12] Electron density difference (EDD) maps could be obtained to provide accurate assignments of excited states by calculating singlet-singlet spin-allowed transitions. Orbital contributions for the selected excited states and orbital composition analysis with Hirshfeld method were all analyzed by Multiwfn software packages.^[12]

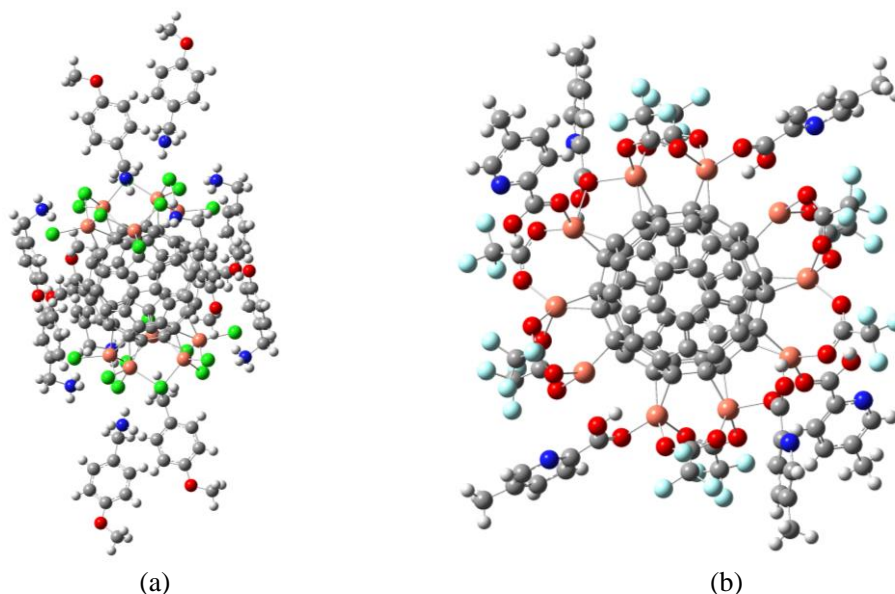


Fig. S6 The calculated decanuclear cuprofullerene model with chemical composition of $[(\text{Cu}^{\text{I}}_5\text{Cl}_{10})(\text{C}_{60})(\text{Cu}^{\text{I}}_5\text{Cl}_{10})]^{10-} \cdot 10(\text{C}_8\text{H}_{12}\text{NO})^+$ (complex **1**, a) and $\text{Cu}^{\text{I}}_{10}\text{C}_{60}(\text{CF}_3\text{COO})_{10}(\text{C}_7\text{H}_7\text{NO}_2)_6$ (complex **2**, b).

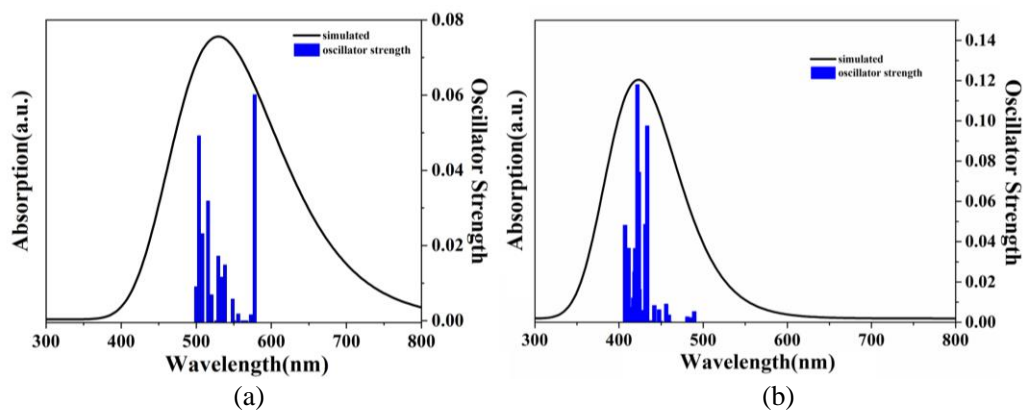
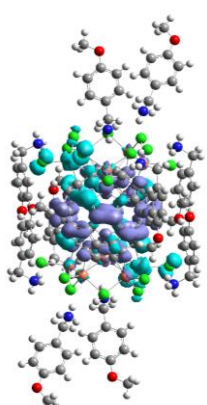
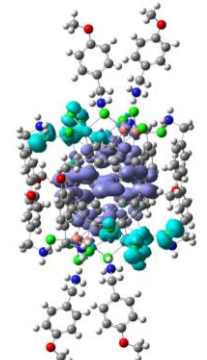
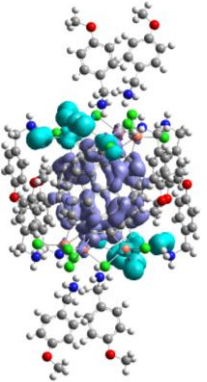
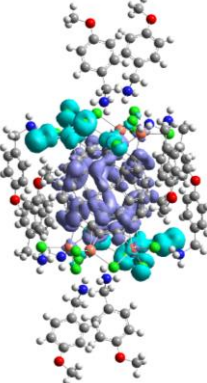
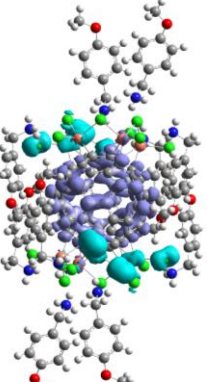
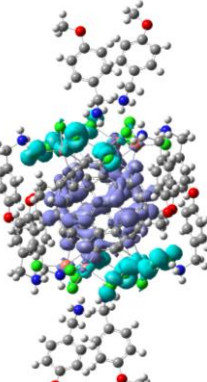
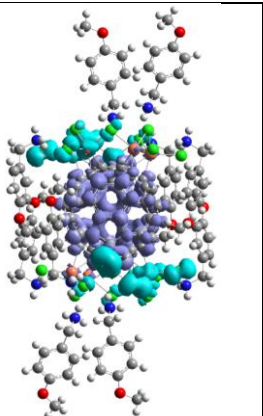
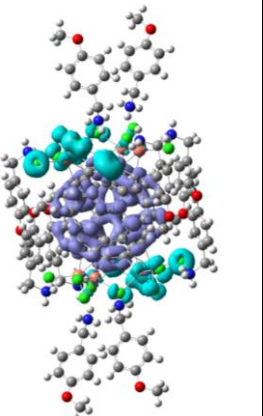


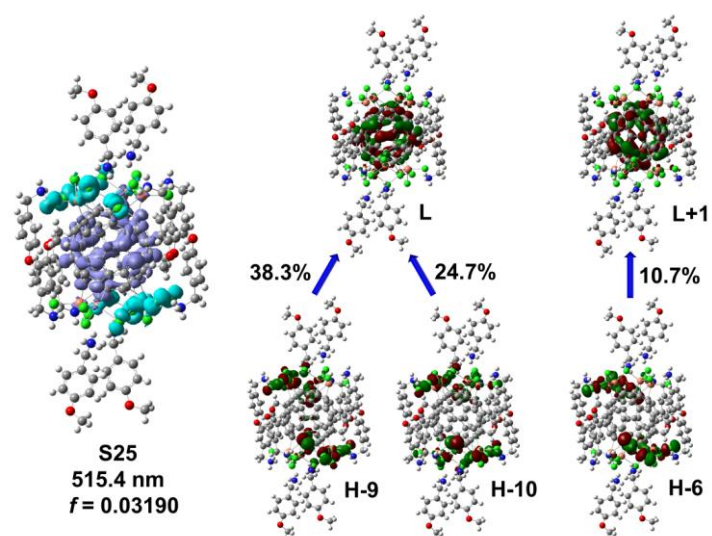
Fig. S7 The calculated absorptions for the model of complexes **1** (a) and **2** (b).

Table S7 The calculated electron density difference (EDD) and the orbital transitions of the vertical singlet excited for complex **1** (isovalue = 0.02).

No.	E(eV)	λ (nm)	f	EDD	Major transitions and contributions (H = HOMO, L = LUMO)
1	1.8830	658.44	0.00000		H \rightarrow L 86.3%
8	2.1450	578.01	0.06010		H-3 \rightarrow L 85.4%, H-4 \rightarrow L 5.6%

16	2.3034	538.27	0.01480		H-4 → L+1 34.3%, H-3 → L+1 32.7%, H-6 → L 10.9%, H-4 → L 7.5%
19	2.3222	533.91	0.01160		H-3 → L+2 71.0%, H-6 → L+1 7.2%
20	2.3431	529.15	0.01720		H-9 → L 27.2%, H-10 → L 13.7%, H-6 → L+1 12.1%, H-6 → L 11.5%, H-3 → L+1 8.3%, H-6 → L+2 7.0%
25	2.4056	515.40	0.03190		H-9 → L 38.3%, H-10 → L 24.7%, H-6 → L+1 10.6%, H-3 → L+2 7.3%, H-9 → L+1 5.2%

27	2.4394	508.26	0.02320		H-6 → L+1 35.1%, H-10 → L 25.9%, H-6 → L+2 14.1%, H-4 → L+2 6.7%
29	2.4615	503.69	0.04920		H-6 → L+2 38.3%, H-12 → L 14.9%, H-9 → L 12.2%, H-10 → L 8.7%



(a)

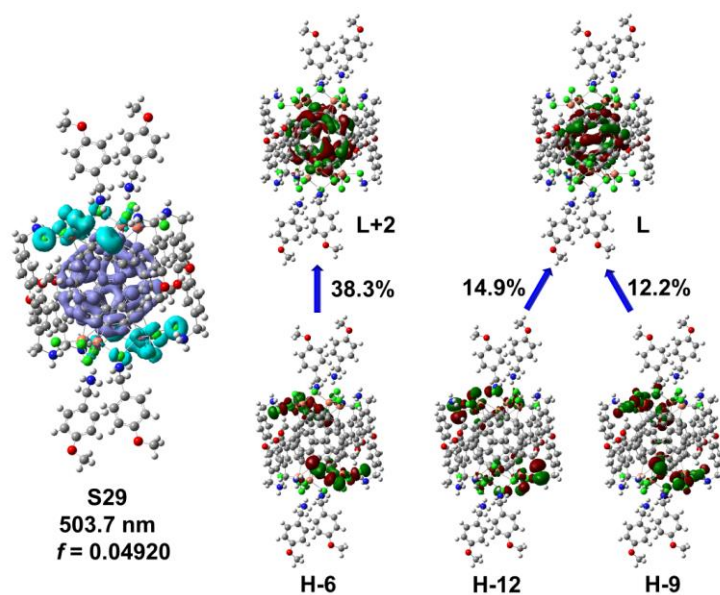
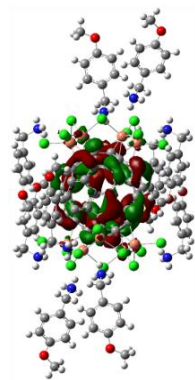


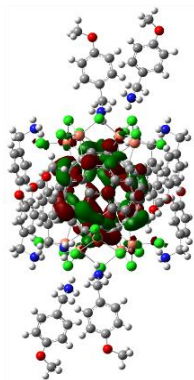
Fig. S8 The calculated photophysical properties of the complex **1** for S25 and S29 states. Left: EDD maps (density transferring from the parts in cyan to purple) of the excited states. Right: spatial plots of the involved molecular orbitals with dominant contributions (H: HOMO, L: LUMO, isovalue = 0.02).

Table S8 The calculated atom/fragment contributions (%) of Cu, Cl and C₆₀ for the selected frontier orbitals of complex **1**.

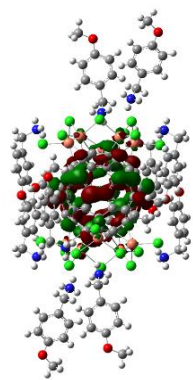
No.	Cu	Cl	C ₆₀
L+2	12.247	5.185	81.320
L+1	12.530	5.558	80.415
L	12.417	4.464	81.072
H	26.803	25.297	46.140
H-1	25.494	23.903	49.163
H-2	31.258	33.284	34.466
H-3	39.864	41.968	16.288
H-4	38.134	51.243	9.361
H-5	31.045	32.401	35.319
H-6	37.494	51.367	9.557
H-7	3.185	3.223	88.896
H-8	31.288	49.674	16.732
H-9	37.690	43.938	17.021
H-10	35.960	51.208	10.040
H-11	23.366	50.190	24.390
H-12	27.785	60.554	9.518
H-13	37.588	47.272	12.751
H-14	31.377	49.412	15.512



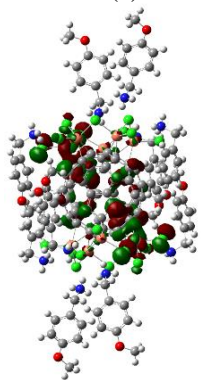
(a) L+2



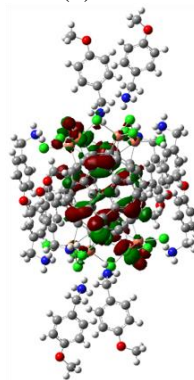
(b) L+1



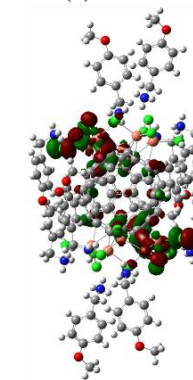
(c) L



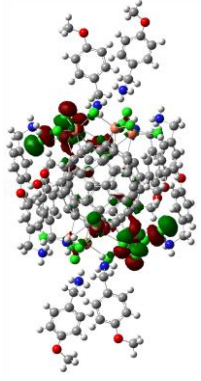
(d) H



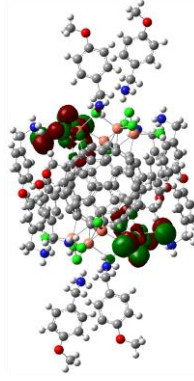
(e) H-1



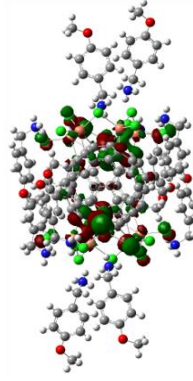
(f) H-2



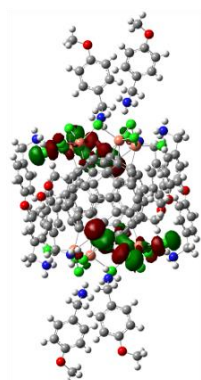
(g) H-3



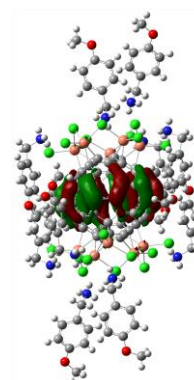
(h) H-4



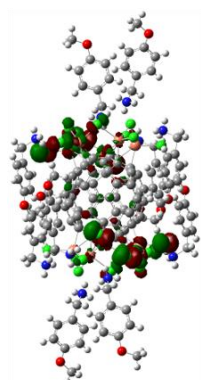
(i) H-5



(j) H-6



(k) H-7



(l) H-8

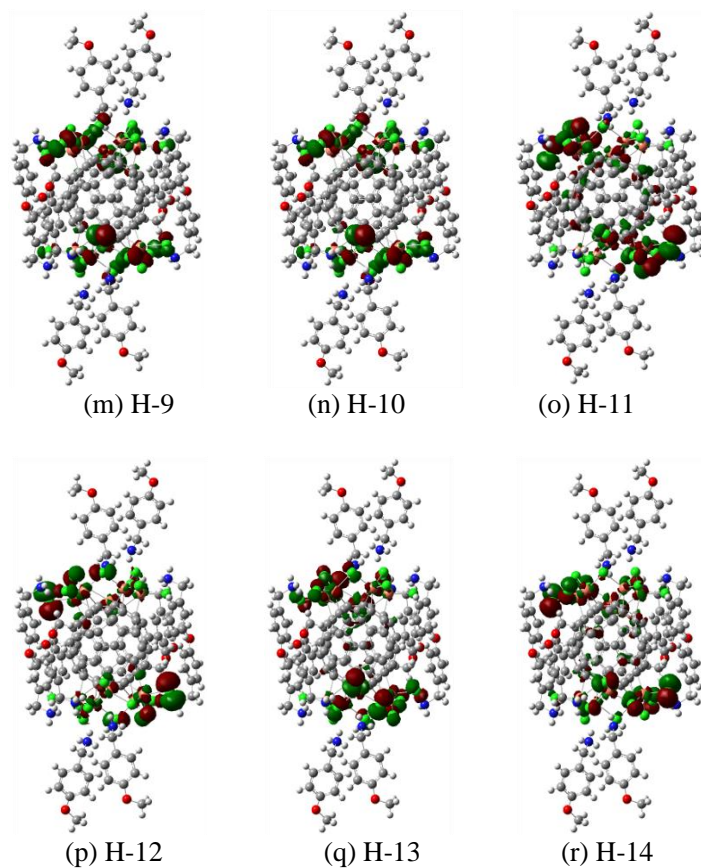
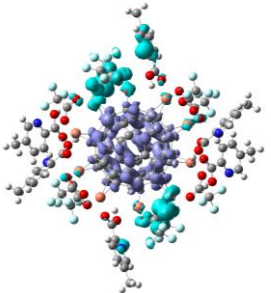
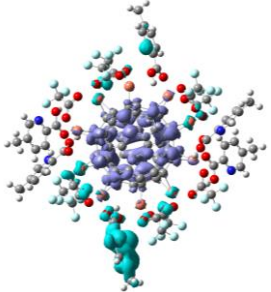
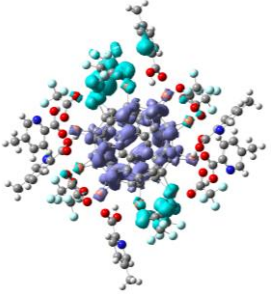
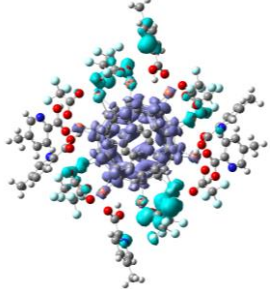
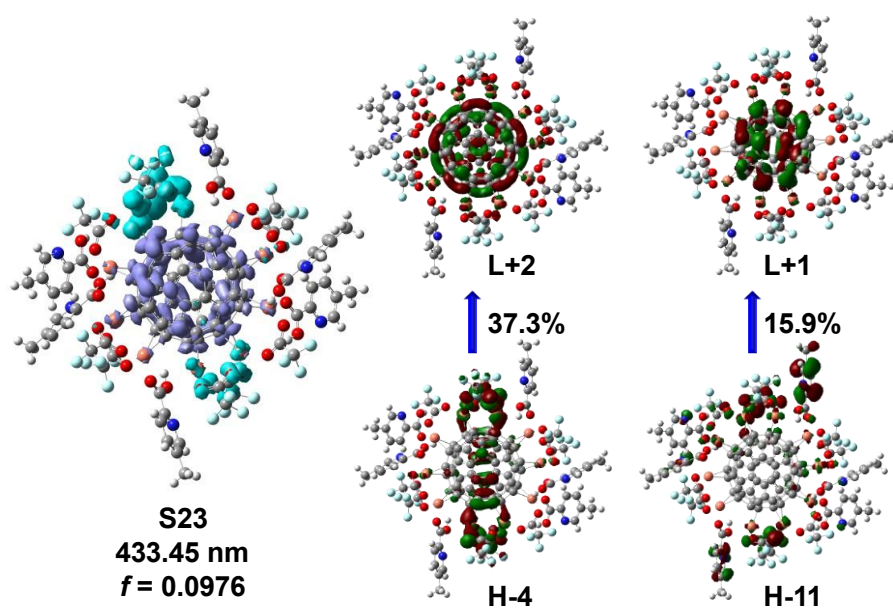


Fig. S9 The contour of HOMO and LUMO for complex **1** (isovalue = 0.02).

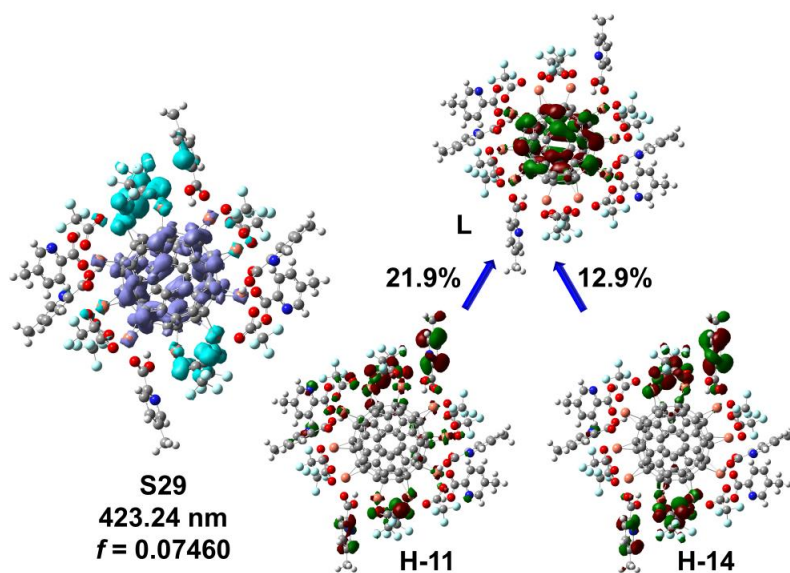
Table S9 The calculated electron density difference (EDD) and the orbital transitions of the vertical singlet excited for complex **2** (isovalue = 0.02).

No.	E(eV)	λ (nm)	f	EDD	Major transitions and contributions (H = HOMO, L = LUMO)
1	1.9615	632.09	0.00000		H \rightarrow L 94.3%
23	2.8604	433.45	0.09760		H-4 \rightarrow L+2 37.3%, H-11 \rightarrow L+1 15.9%, H-14 \rightarrow L+1 8.9%, H-16 \rightarrow L+1 5.2%

24	2.8728	431.58	0.04860		<p>H-11 → L+1 19.5%, H-4 → L+2 19.1%, H-14 → L+1 10.3%, H-11 → L 8.4%, H-5 → L+2 5.7%, H-6 → L 5.5%</p>
28	2.9219	424.33	0.01630		<p>H-7 → L 39.8%, H-5 → L+2 11.5%, H-9 → L 9.1%, H-13 → L 7.2%, H-8 → L+2 6.1%</p>
29	2.9294	423.24	0.07460		<p>H-11 → L 21.9%, H-14 → L 12.9%, H-5 → L+2 11.1%, H-11 → L+1 7.0%, H-4 → L+2 6.3%, H-8 → L+2 5.4%</p>
30	2.9390	421.86	0.11810		<p>H-5 → L+2 24.8%, H-11 → L 10.8%, H-14 → L 9.3%, H-6 → L+1 8.7%, H-13 → L 5.9%</p>



(a)



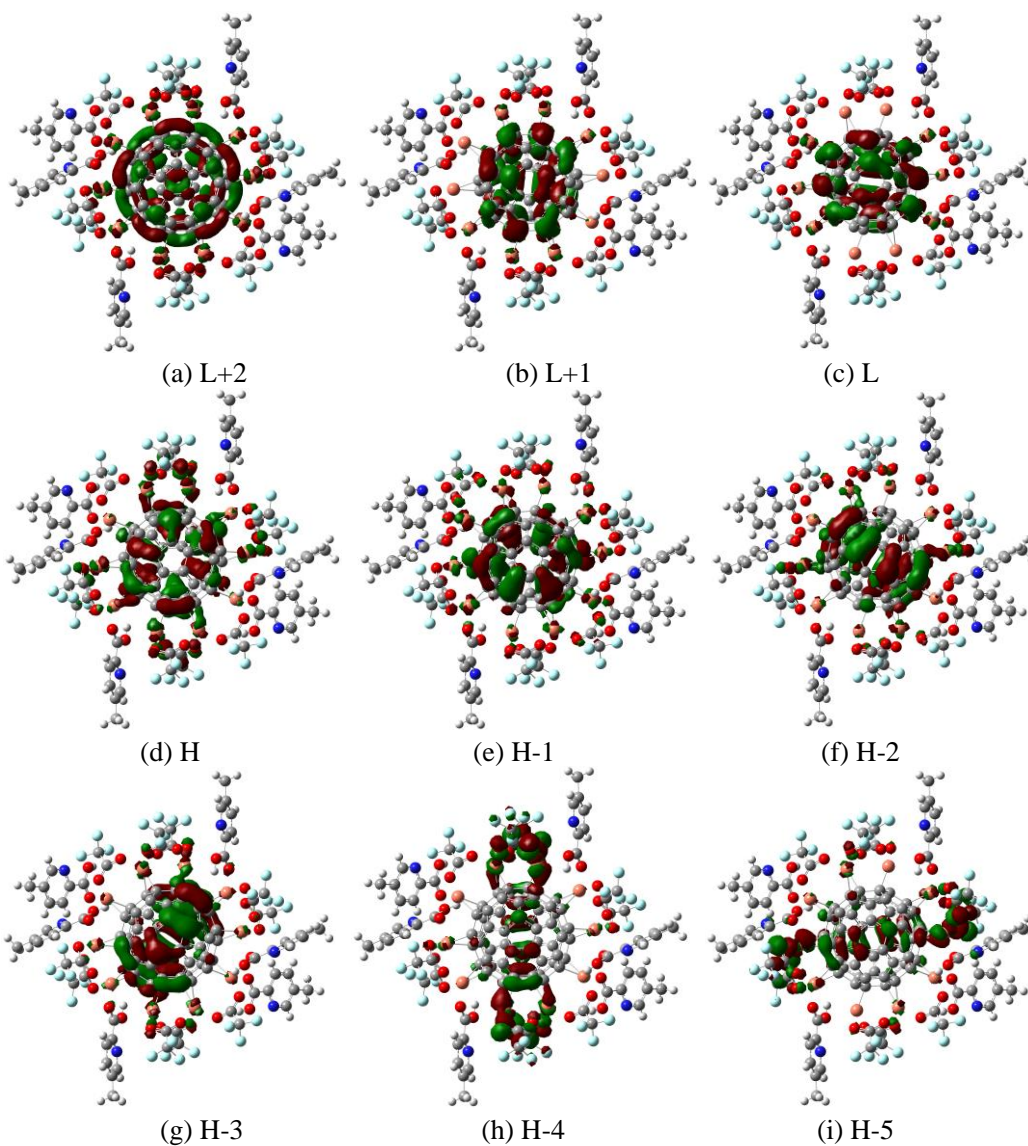
(b)

Fig. S10 The calculated photophysical properties of complex **2** for S23 (a) and S29 (b) states. Left: EDD maps (density transferring from the parts in cyan to purple) of the excited states. Right: spatial plots of the involved molecular orbitals with dominant contributions (H: HOMO, L: LUMO, isovalue = 0.02).

Table S10 The calculated atom/fragment contributions (%) of Cu, N, O and C₆₀ for the selected frontier orbitals of complex **2**.

No.	Cu	N	O	C ₆₀
L+2	25.062	0.018	5.998	66.827
L+1	7.922	0.011	1.868	89.468
L	8.386	0.021	2.084	88.233
H	19.436	0.048	10.670	65.723
H-1	19.187	0.226	7.736	70.261
H-2	13.661	0.338	7.279	76.310

H-3	11.189	0.230	5.466	81.071
H-4	27.713	0.140	28.452	30.146
H-5	31.818	0.949	24.382	32.098
H-6	5.157	43.978	10.080	5.493
H-7	6.419	42.228	10.514	6.916
H-8	23.881	7.627	35.261	15.770
H-9	21.383	20.634	15.952	25.283
H-10	1.948	55.993	5.048	2.114
H-11	16.555	5.951	30.415	10.837
H-12	5.143	48.961	8.021	4.730
H-13	18.755	13.488	20.261	15.106
H-14	16.656	4.155	27.090	6.822



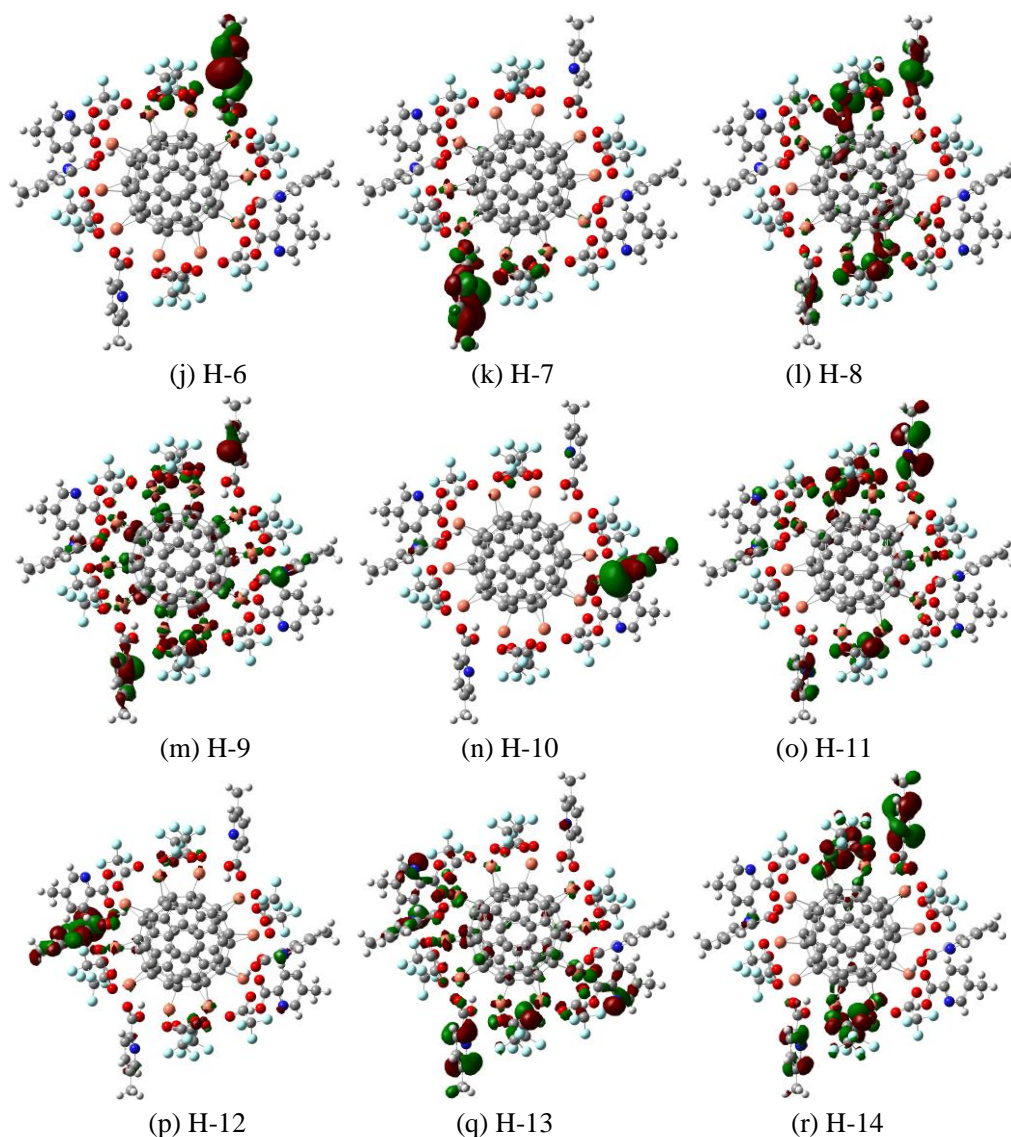


Fig. S11 The contour of HOMO and LUMO for complex **2** (isovalue = 0.02).

4. References

- [1] a) G. M. Sheldrick, A short history of SHELX. *Acta Cryst.*, **2008**, *A64*: 112–122. b) M. Sheldrick, Crystal structure refinement with SHELXL, *Acta Crystallogr., Sect. C: Cryst. Struct. Commun.*, 2015, **71**, 3-8.
- [2] O. V. Dolomanov, L. J. Bourhis, R. J. Gildea, J. A. K. Howard, H. Puschmann. OLEX2: a complete structure solution, refinement and analysis program. *J. Appl. Cryst.*, **2009**, *42*, 339–341.
- [3] M. J. Frisch, *et al.*, Gaussian 16, Gaussian, Inc., Wallingford CT, 2016.
- [4] a) J. P. Perdew, K. Burke and M. Ernzerhof, Generalized Gradient Approximation Made Simple, *Phys. Rev. Lett.*, 1996, **77**, 3865-3868. b) C. Adamo and V. Barone, Inexpensive and accurate predictions of optical excitations in transition-metal complexes: the TDDFT/PBE0 route, *Theor. Chem. Acc.*, 2000, **105**, 169-172.
- [5] P. J. Hay and W. R. J. Wadt, Ab *initio* effective core potentials for molecular calculations. Potentials for the transition metal atoms Sc to Hg., *J. Chem. Phys.*, 1985, **82**, 270-283.

- [6] a) P. J. Hay and W. R. Wadt, Ab initio effective core potentials for molecular calculations. Potentials for K to Au including the outermost core orbitals, *The Journal of Chemical Physics*, 1985, **82**, 299-310. b) R. C. Binning Jr and L. A. Curtiss, Compact contracted basis sets for third-row atoms: Ga–Kr, *J. Comput. Chem.*, 1990, **11**, 1206-1216.
- [7] T. Lu and F. Chen, Multiwfn: A multifunctional wavefunction analyzer, *J. Comput. Chem.*, 2012, **33**, 580-592.